

# Heptad-repeat-2 mutations enhance the stability of the enfuvirtide-resistant HIV-1 gp41 hairpin structure

*Ekachai Jenwitheesuk and Ram Samudrala\**

Department of Microbiology, University of Washington School of Medicine, Seattle, WA 98195, USA

\*Corresponding author: Tel: +1 206 732 6122; Fax: +1 206 732 6055; E-mail: ram@compbio.washington.edu

Enfuvirtide (T20) is a peptide-based fusion inhibitor derived from the heptad repeat 2 (HR2) region of HIV-1 glycoprotein 41 (gp41). The inhibitor binds to the gp41 heptad repeat 1 (HR1) region, thereby blocking viral HR1/HR2 association. Mutations in HR1 have been reported to cause enfuvirtide resistance and reduce viral fitness. In this study, we first showed that scores obtained by a residue-specific all-atom probability discriminatory function (RAPDF) may be used as a reliable predictor of structural stability of gp41 mutants by comparing it to experimentally determined melting temperatures, and as a reliable indicator of enfuvirtide resistance by comparing it to experimentally determined fusion inhibition and viral fitness levels. We then generated an initial set of 28 theoretical structures of the HR1/HR2 hairpin complex where each structure consists of one mutation on HR1 known to

cause enfuvirtide resistance and a wild-type amino acid at the corresponding HR2 residue. Mutations were then introduced in the corresponding HR2 residue of each structure where the wild-type amino acid was changed to each of the other nineteen amino acids. The enfuvirtide-resistant HR1 mutants with compensatory mutations at the corresponding HR2 residues had better RAPDF scores than those HR1 mutants with wild-type HR2. This indicates that mutations in HR2 improve structural stability of the HR1/HR2 hairpin complex and may lead to enhanced enfuvirtide resistance when present with resistant HR1 mutations. Modification of the amino acid side chains that contribute to enfuvirtide resistance using the RAPDF scores as a guide may help design of a second generation of fusion inhibitors against the enfuvirtide-resistant strains.

## Introduction

Glycoprotein 41 (gp41) is a crucial molecule in the human immunodeficiency virus type 1 (HIV-1) envelope and consists of four major parts: an amino-terminal hydrophobic fusion peptide, a cysteine loop, and heptad repeats 1 and 2 (HR1 and HR2). gp41 mediates fusion of viral and target-cell membranes by inserting its fusion peptide into the target-cell membrane after formation of CD4/gp120/chemokine-receptor complex. The HR1 trimer is a three-stranded coiled-coil structure that associates with HR2 in an antiparallel orientation to form a six-helical bundle hairpin complex. Formation of the HR1/HR2 hairpin complex brings viral and target-cell membranes in close proximity to enable membrane fusion and viral entry (Figure 1) [1–3].

Enfuvirtide is the first approved peptide-based HIV-1 fusion inhibitor. It corresponds to amino acid residues 127–162 of HIV-1 gp41 (part of the HR2 domain) or residues 643–678 in the gp160 precursor of the HIV envelope glycoprotein. The inhibitor competes with the viral HR2 in binding to the HR1 trimeric coiled-coil hydrophobic groove, thereby blocking viral HR1/HR2 association [4–7].

Mutations of HR1 residues at the hydrophobic groove (G36, V38, Q40, N42, N43 and L45) have been reported to cause enfuvirtide resistance [8–10]. Although HIV-1 strains with these HR1 mutations can escape from enfuvirtide, these strains are significantly less fit than the wild-type strains [10–12]. It is unclear how viral HR1 and HR2 mutations reduce the effectiveness of the enfuvirtide and whether these mutations subsequently restore viral fitness.

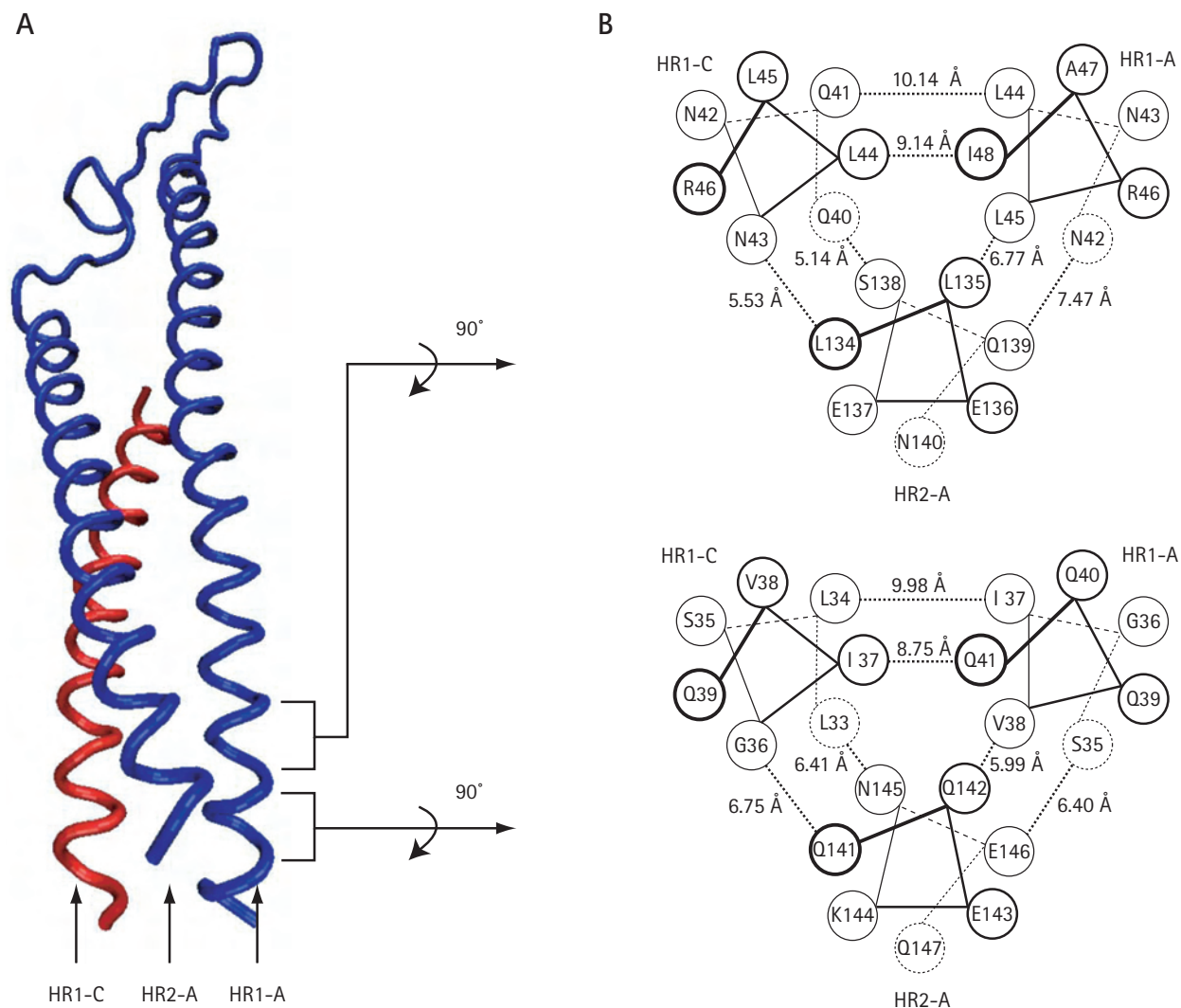
In this study, we used a computational protein modelling approach to investigate the effects of amino acid changes in HR2 at positions that directly interact with the enfuvirtide-resistant HR1 residues. We show that such changes in HR2 improve the structural stability of the HR1/HR2 hairpin complex, thereby enhancing drug resistance level and viral fitness of the enfuvirtide-resistant strains.

## Materials and methods

### Generation of mutant theoretical structures

The theoretical structure of a six-helical bundle HIV-1 gp41 hairpin complex consisting of HR1, HR2 and the

Figure 1. The HIV-1 gp41 structure used in this study is a six-helical bundle hairpin complex consisting of three chains (A, B and C)



Each chain consists of three parts: HR1, HR2 and cysteine loop. (A) The HR1 domains in chain C (HR1-C) and chain A (HR1-A) form a coiled-coil structure that allows HR2 of chain A (HR2-A) to bind in an antiparallel orientation. Enfuvirtide, a synthetic peptide that structurally mimics HR2, inhibits viral and target cell membrane fusion by competitively binding with the HR1 and blocking HR1/HR2 association. (B) Mapping of residue-residue interactions between HR1 and HR2 was carried out by defining HR2 residues with  $C\alpha$ - $C\alpha$  distances  $<7.5$  Å from the following HR1 residues: G36, V38, Q40, N42, N43 and L45. The mapping diagrams show the top view of HR1-A/HR2-A/HR1-C complex. The residue number and the wild-type amino acid code of each residue are labelled in circle connected by lines that illustrate the sequence order. The shortest  $C\alpha$ - $C\alpha$  distance between interacting residues is given.

cysteine loop (Protein Data Bank identifier 1IF3) was used as a template for creating mutant structures. This structure was previously modelled using NMR restraints from the simian immunodeficiency virus (SIV) gp41 ectodomain as a template [13]. Wild-type side chains were substituted with the mutant side chains based on a backbone-dependent side chain rotamer library and a linear repulsive steric energy term provided by SCWRL version 3.0 [14]. The resulting all-atom models were energy minimized for 200 steps using the Energy Calculation and Dynamics (ENCAD) program [15–18].

#### Prediction of the stability of the hairpin complex structures

A residue-specific all-atom probability discriminatory function (RAPDF) score [19] was used as an indicator of the structural stability of a given hairpin complex. This function has been used as a key component of protein structure prediction methods that work well in the CASP blind prediction experiments [20].

The RAPDF score was used as a proxy for the structural stability of a given hairpin complex. The RAPDF score is calculated based on the conditional probability of a conformation being native-like given

a set of interatomic distances. The conditional probabilities are compiled by counting frequencies of distances between pairs of atom types in a database of protein structures. The distances observed are divided into 1.0 Å bins ranging from 3.0 Å to 20.0 Å. Contacts between atom types in the 0–3 Å range are placed in a separate bin, resulting in a total of 18 distance bins. Distances within a single residue are not included in the counts. We compiled tables of scores proportional to the negative log conditional probability that one is observing a native conformation given an interatomic distance for all possible pairs of the 167 atom types for the 18 distance ranges from a database of known structures. Given a set of distances in a conformation, the probability that the conformation represents a correct fold is evaluated by summing the scores for all distances and the corresponding atom pairs. A complete description of this formalism has been published elsewhere [19].

#### Comparison of the RAPDF stability scores with experimentally determined melting temperatures

We generated a set of ten gp41 mutant structures for which the melting temperatures ( $T_m$ ) are available [21,22]. The RAPDF scores for these structures and the wild-type structure was calculated and compared to the melting temperatures (Table 1). The goal was to determine how well the predicted RAPDF scores correlate with experimentally determined gp41 stability.

#### Comparison of the RAPDF stability scores with the $EC_{50}$ values and the viral fitness levels

We generated a set of seven HR1-mutant/HR2-wild-type structures for which the  $EC_{50}$  values (the molar

concentrations of enfuvirtide that inhibits viral-target cell membrane fusion by 50%) [23] and the viral fitness levels [11] are available (Table 2). The second set of these mutants was duplicated from the first set with additional HR2 compensatory mutations (S138Y and Q139R). We calculated the RAPDF scores for the structures in both sets and compared the scores with the experimental enfuvirtide  $EC_{50}$  values and the viral fitness levels. The goal was to determine how well the RAPDF scores (and, by inference, protein stability) predict  $EC_{50}$  and viral fitness.

#### Mapping of HR1/HR2 residue-residue interactions

We mapped the HR1/HR2 residue-residue interactions by finding the corresponding HR2 residues that had  $C\alpha$ - $C\alpha$  distances within 7.5 Å from the following enfuvirtide-resistant HR1 residues: G36, I37, V38, Q40, N42, N43, L44 and L45 (Figure 1) [8, 10].

#### Generation of enfuvirtide-resistant HR1/HR2 hairpin structures

We generated an initial set of 28 mutant structures of the HR1/HR2 hairpin complex such that each structure consisted of one enfuvirtide-resistant mutation on HR1 and a wild-type amino acid at the corresponding HR2 residue. This initial set was used to generate nineteen other sets of HR1/HR2 double mutants such that the corresponding HR2 wild-type residue was changed to each of the remaining nineteen amino acids. At the end of this step, we obtained a total of 560 structures of the enfuvirtide-resistant HR1/HR2 mutant complex. The mutation patterns of the generated hairpin structures are shown in Figure 2.

**Table 1.** Correlation of the RAPDF scores and the corresponding melting temperatures for 10 HR1 or HR2 single mutants, as well as the wild-type, from two sources [21,22]

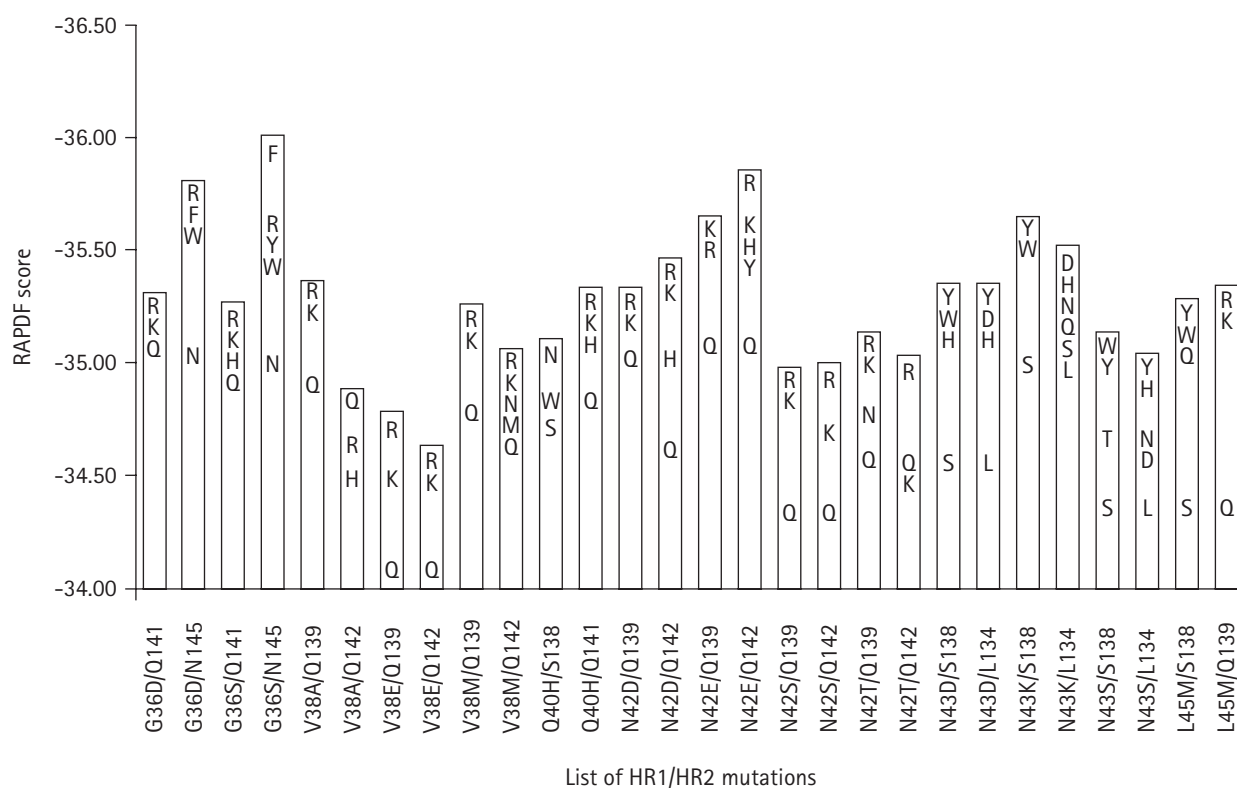
Mutation	Melting temperature (°C)	RAPDF score	References
Wild type	76	-35.12	21
I48G	46	-33.14	21
I48P	34	-33.26	21
L55V	72	-34.40	21
T58P	44	-34.26	21
Wild type	78	-35.12	22
I62A	55	-34.14	22
I62P	40	-34.03	22
I62S	51	-34.21	22
I62V	71	-34.46	22
I131A	71	-34.38	22
I131S	67	-34.47	22

The correlation coefficient is 0.82 (0.86 when the single outlier [I62P] is removed) showing that as the residue-specific all-atom probability discriminatory function (RAPDF) score increases (that is, indicating lower stability), the melting temperature decreases.

**Table 2.** Correlation of the RAPDF scores, the enfuvirtide EC<sub>50</sub> values and the viral fitness levels

HR1 mutation	Viral fitness level	EC <sub>50</sub> (mg/l)	RAPDF score	
			HR2 wild type	With HR2 mutation
Wild type	+++++	0.012	-35.12	-
N42T	++++	0.045	-34.66	-35.13 (Q139R)
V38A	+++	0.188	-34.98	-35.36 (Q139R)
N42T+N43K	++	0.388	-34.69	-36.21 (S138Y, Q139R)
N42T+N43S	++	0.727	-34.65	-35.66 (S138Y, Q139R)
V38A+N42D	+	1.685	-34.89	-35.42 (Q139R)
V38A+N42T	+	1.782	-34.49	-35.13 (Q139R)
V38E+N42S	Data not available	6.156	-33.73	-35.02 (Q139R)

The residue-specific all-atom probability discriminatory function (RAPDF) scores of the HR1 mutant structures range from -34.98 to -33.78, which are higher than that of the wild-type (-35.12). The scores directly correlate with the previously published EC<sub>50</sub> values [23] and inversely correlate with the viral fitness levels (represented by the + symbol) [11]. The correlation coefficient between the RAPDF scores and the EC<sub>50</sub> values is 0.9. After amino acid substitutions at positions 138 and 139 in HR2, the RAPDF scores of the HR1 mutant structures range from -36.21 to -35.02, indicating that compensatory HR2 mutations improve the structural stability of the HR1/HR2 hairpin complexes.

**Figure 2.** List of enfuvirtide-resistant HR1 mutants and the corresponding HR2 residues

The amino acid codes in each bar are the compensatory amino acids at the corresponding HR2 positions predicted to improve structural stability of the hairpin complex. The height of the amino acid code represents the RAPDF score of the HR1/HR2 hairpin complex. The lower the RAPDF score the higher the structural stability of the hairpin complex.

Identification of the amino acids at the corresponding HR2 positions that improve structural stability of the hairpin complex

The RAPDF scores of 560 HR1/HR2 mutant structures calculated from the previous step were compiled in a 28×20 table. Each row of this table contains 20 RAPDF scores calculated from 20 hairpin structures. Each of these 20 hairpin structures consisted of one enfuvirtide-resistant mutation on HR1 and one of the 20 amino acids at the corresponding HR2 residue. We identified the amino acid at the corresponding HR2 residue that improved structural stability of the hairpin complex by calculating the mean and standard deviation of the RAPDF scores on each row. The cut-off was set at one standard deviation under the mean. The hairpin structure that had the RAPDF score lower than the cut-off was defined as having improved structural stability. The amino acid at the corresponding HR2 residue of this structure was defined as a ‘compensatory amino acid’ that improved the structural stability of the hairpin complex (Figure 2).

Designing enfuvirtide derivatives against enfuvirtide-resistant strains

From the mapping of residue–residue interactions and the identification of HR2 compensatory amino acid studies, we identified six corresponding HR2 residues (134, 138, 139, 141, 142 and 145) that were in close contact with the enfuvirtide-resistant HR1 residues. The HR2 compensatory amino acids identified based on the RAPDF scores were: D, H, (L), N, Q, S, Y for residue 134; H, N, Q, (S), T, W, Y for residue 138; K, N, (Q), R for residue 139; H, K, R, (Q) for residue 141; H, K, M, N, (Q), R, Y for residue 142 and F, (N), R, W, Y for residue 145. (Wild-type amino acids are indicated by parenthesis.)

We generated an initial set of eighteen HR1 mutant structures reported to cause enfuvirtide resistance in patients [8–10]. The list of the HR1 mutations is shown in Table 2. For each HR1 mutant structure, we introduced mutations at residues 134, 138, 139, 141, 142 and 145 of the HR2. The wild-type amino acids of these six HR2 residues were randomly replaced by the compensatory amino acids. This yielded a total of 27,440 HR1/HR2 mutant structures, each of which had different HR2 mutation patterns. The same procedure was applied to all eighteen HR1 mutant structures so that we obtained a total of 493,920 HR1/HR2 mutant structures in this step.

All structures were constructed as previously described scored using the RAPDF function. We categorized the RAPDF scores into eighteen groups according to eighteen HR1 mutation patterns. The

scores were ranked in ascending order to find the general patterns of HR2 mutations that could stabilize hairpin complexes of all enfuvirtide-resistant mutants (Table 3).

## Results and discussion

Comparison of the RAPDF stability scores with experimentally determined melting temperatures

Table 1 shows the RAPDF stability scores and the corresponding melting temperatures for 10 HR1 or HR2 single mutants, as well as the wild type, from two sources [21,22]. The correlation coefficient is 0.82 (0.86 when the single outlier [I62P] is removed) showing that as the RAPDF score increases (that is, indicating lower stability), the melting temperature decreases. The best score is obtained for the wild type (which also has the highest melting temperature reported in both sources). This result indicates that the RAPDF score, a key component of protein structure prediction methods that work well [20], may be used as a predictor of structural stability.

Comparison of the RAPDF stability scores with the EC<sub>50</sub> values and the viral fitness levels

We compared the RAPDF scores of seven HR1 mutants with the EC<sub>50</sub> values of enfuvirtide and the viral fitness levels. Table 2 shows that the wild type structure had the best RAPDF score (-35.12). The scores increased to range from -34.98 to -33.78 for all seven HR1 mutant structures and were directly correlated with the EC<sub>50</sub> values and inversely correlated with the viral fitness levels. The correlation coefficient between the RAPDF scores and the EC<sub>50</sub> values was 0.9 (Table 2). This result indicates that our structural stability scores may be used to accurately estimate the viral fitness levels and the inhibitory activity of the enfuvirtide and its derivatives.

Mapping of HR1/HR2 residue–residue interactions

We considered structural arrangement of eight HR1 residues (G36, I37, V38, Q40, N42, N43, L44 and L45) that have been associated with enfuvirtide resistance [8–10]. Figure 1 illustrates that all eight residues are in the hydrophobic groove of the HR1, where I37 and L44 form the bottom of the groove and G36, V38, Q40, N42, N43 and L45 form the binding surface for the HR2 domain. Mapping of HR1/HR2 residue–residue interaction revealed six corresponding HR2 residues (L134, S138, Q139, Q141, Q142 and N145) that interact with the binding surface of the HR1 with Cα–Cα distances <7.5 Å. The side chains of these corresponding HR2 residues are in close contact with the eight HR1 residues except those between L45 and I135. Their side chains do not interact with each

other, though the  $C\alpha$ - $C\alpha$  distance was 6.77 Å. The side chain of L45 is in between S138 and Q139, whereas the side chain of I135 points toward Q52 (Figure 1).

#### Identification of the amino acids at the corresponding HR2 positions that improve structural stability of the hairpin complex

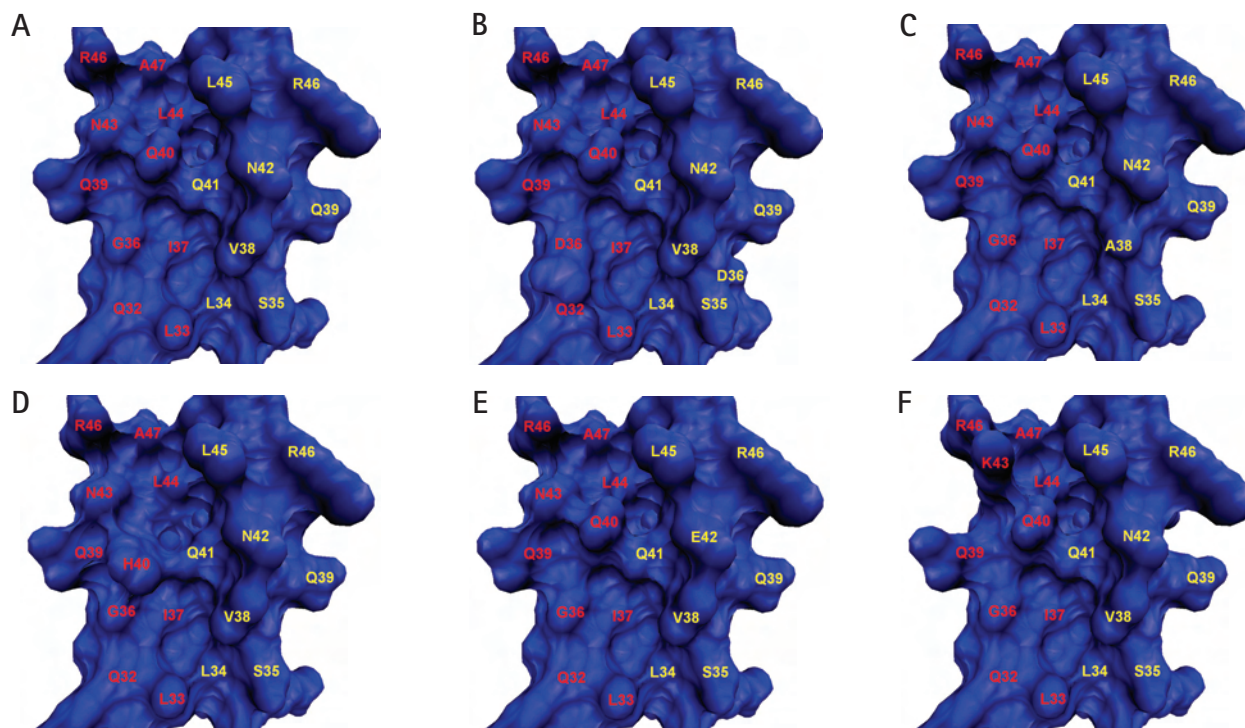
We calculated the RAPDF scores of the enfuvirtide-resistant HR1 mutant structures (G36D/S, V38A/E/M, Q40H, N42D/E/S/T, N43D/K/S and L45M) and compared them to the wild-type structure score. The RAPDF scores for these mutant structures ranged from -35.06 to -34.09, which were higher than the score of the wild-type structure (-35.12). This indicates that the enfuvirtide-resistant mutants have lower hairpin structural stability than the wild-type strains.

The residue-residue mapping revealed six corresponding HR2 residues that interact with eight enfuvirtide-resistant HR1 residues. We then hypothesized that the compensatory amino acid substitutions at these corresponding HR2 residues may improve structural stability of the HR1/HR2 hairpin complex. To identify these compensatory amino acids, we replaced the wild-type amino acid at the corresponding HR2

positions with each of the other nineteen amino acids. The RAPDF scores of these HR1/HR2 mutant structures indicated that the HR2 compensatory amino acids were as follows: D, H, (L), N, Q, S, Y for residue 134; H, N, Q, (S), T, W, Y for residue 138; K, N, (Q), R for residue 139; H, K, R, (Q) for residue 141; H, K, M, N, (Q), R, Y for residue 142; and F, (N), R, W, Y for residue 145. (Wild-type amino acids are indicated by parenthesis.) The RAPDF scores of the HR1 mutants possessing one of these HR2 compensatory amino acids ranged from -36.01 to -34.11, indicating enhancement of the structural stability of the hairpin complex after introducing the compensatory amino acids at the corresponding HR2 positions (Figure 2).

We further tested whether the HR2 compensatory mutations improve the structural stability of these seven hairpin complexes. The results from residue-residue interaction and compensatory amino acid identification studies suggest that Q139R and/or S138Y mutations in the HR2 are likely to improve the RAPDF scores for these HR1 mutants. Therefore, we introduced the Q139R mutation in all the HR1 mutant structures with an additional S138Y mutation for the N42T+N43K and N42T+N43S mutant structures.

Figure 3. Surface structures of the hydrophobic groove formed by the HR1 domains of chain A and chain C



Comparison of the surface structures of the wild-type (A), G36D (B), V38A (C), Q40H (D), N42E (E) and N43K (F) mutants shows prominent changes at the HR1 grooves of G36D, Q40H and N43K mutants. The amino acids and numbers of HR1 chain A and chain C are labelled in yellow and red, respectively.

**Table 3.** List of enfuvirtide-resistant mutations and amino acid substitutions at six HR2 residues that improve structural stability of the HR1/HR2 hairpin complexes

HR1 mutation	HR2 mutation (residues 134,138, 139,141,142,145)	RAPDF score
Wild type	Wild type	-35.12
Wild type	H Y R R R Y	-37.92
Wild type	----- F	-37.01
Wild type	----- R	-37.28
G36D	----- F	-37.85
G36S	----- F	-38.01
V38A	----- F	-37.97
V38A+N42D	----- F	-38.44
V38A+N42T	----- F	-37.81
V38E+N42S	----- R	-36.71
V38E	- N --- R	-37.16
V38M	-----	-37.86
Q40H	-----	-37.88
N42D	-----	-38.50
N42E	-----	-38.69
N42S	-----	-37.75
N42T	-----	-37.76
N42T+N43S	-----	-37.55
N43D	-----	-38.11
N43K	-- K ---	-37.94
N43S	-----	-37.65
L45M	-----	-37.92

Enfuvirtide derivative designed according to these HR2 mutation patterns may have high structural stability against both wild-type and enfuvirtide-resistant strains. The amino acid code in a column that is identical to the first sequence is represented by the (-) symbol.

We found that these two HR2 compensatory mutations improved the RAPDF scores of all seven HR1 mutants (ranging from -36.21 to -35.02).

### Mechanism of enfuvirtide resistance

Our theoretical structural stability scoring suggests a possible enfuvirtide-resistance mechanism: initially, mutations in HR1 may be selected to reduce structural stability of HR1/enfuvirtide complex. These mutations alter the biochemical properties (for example, polarity and hydrophobicity) and modify the conformation of the HR1 coiled-coil hydrophobic groove. Comparison of the side chain arrangement at the binding surface of wild-type and mutant HR1 grooves shows that conformational changes are prominent in G36D, Q40H and N43K mutations (Figure 3). These changes limit binding site access of enfuvirtide, resulting in increased EC<sub>50</sub> values. However, these mutants have low viral fitness because the mutations of the HR1 also reduce structural stability of the HR1/HR2 hairpin complex. Compensatory mutations at the corresponding HR2 residues are then selected to enhance structural stability

of HR1/HR2 complex, thereby improving viral fitness and destabilizing the HR1/enfuvirtide complex.

Even though we are unable to make a direct comparison between the increased theoretical stability of compensatory HR2 mutations and a corresponding increase in experimentally determined melting temperatures, we have demonstrated that the RAPDF score is a reliable indicator of melting temperatures for an independent set of mutations (Table 1). In addition, we have also shown that the RAPDF score is a reliable indicator of the EC<sub>50</sub> and viral fitness levels (Table 2). Taken together, these results indicate that decreased stability of HR1 mutants (predicted by RAPDF scores that correlate well with experimentally determined melting temperatures) is reversed by the compensatory HR2 mutants (as predicted by RAPDF), which in turn results in lower fusion inhibition and increased viral fitness (RAPDF scores also correlate well with these experimental measures of enfuvirtide activity). Our predictions and results are consistent with previously observed correlations between melting temperatures of the HR1/HR2 complex and fusion inhibition [24].

### Designing enfuvirtide derivatives against enfuvirtide-resistant strains

Previous experimental and clinical studies have identified eighteen mutation patterns in HR1 that are implicated in enfuvirtide resistance in patients [8–10]. In this study, we identified six corresponding HR2 residues and the compensatory amino acids that have a role in improving structural stability of the enfuvirtide-resistant hairpin complex. This suggests the possibility of designing enfuvirtide derivatives to inhibit these resistant strains.

To find the best derivative, we generated eighteen enfuvirtide-resistant HR1 mutant structures. For each HR1 mutant structure, the wild-type amino acids at six corresponding HR2 residues were randomly replaced by the compensatory amino acids, yielding 27,440 HR1/HR2 mutant structures, each with a different HR2 mutation pattern. Finally, we obtained a total of 493,920 HR1/HR2 mutant structures after applying this procedure to all eighteen HR1 mutants.

Of the 493,920 mutant structures generated, we found a common HR2 mutation pattern that improved the RAPDF scores of all eighteen enfuvirtide-resistant strains; that is, L134H, S138Y, Q139R, Q141R, Q142R, N145Y/F/R. The scores ranged from -38.69 to -36.71, which were better than that of the HR1/HR2 wild-type strain (Table 3). This finding suggests a list of the amino acids that may be used to design enfuvirtide derivatives. Modification of the enfuvirtide molecule should focus at the six corresponding residues with amino acid side chains replaced by the ones suggested in Table 3. Such a modification enhances interaction of

the derivatives against the wild-type strain and the enfuvirtide-resistant mutants.

## Conclusion

In this study, we applied a RAPDF to score theoretical models of HIV-1 gp41 to demonstrate that the mutant enfuvirtide-resistant strains have low structural stability. The RAPDF scores of these resistant mutants improved after amino acid substitutions at the corresponding residues of HR2 that interact with the HR1 mutant. Our findings suggest an enfuvirtide resistance mechanism: mutations of HR1 modify the hydrophobic groove that limits the likelihood of enfuvirtide accessing its binding site. Additional mutations at the corresponding HR2 residues improve structural stability of the HR1/HR2 hairpin complex, thereby enhancing viral fitness of the mutant strains. This resistance mechanism leads to the idea of designing novel enfuvirtide derivatives that may compete with the viral HR2 for binding in the modified HR1 hydrophobic groove. A combination of such enfuvirtide derivatives along with the HR1-derived enfuvirtide-complement peptide (and its derivatives) may have high potency in reducing viral load and have a wide spectrum effect in controlling HIV-1 wild-type as well as fusion-inhibitor-resistant strains.

## Acknowledgements

This work was supported in part by NIH grant GM068152, NSF grant DBI-0217241, a NSF CAREER award, and a Searle Scholar Award to Ram Samudrala. The authors would like to thank members of the Samudrala group for valuable discussions and comments.

## References

- Wyatt R & Sodroski J. The HIV-1 envelope glycoproteins: fusogens, antigens, and immunogens. *Science* 1998; 280:1884–1888.
- Chan DC & Kim PS. HIV entry and its inhibition. *Cell* 1998; 93:681–684.
- Weissenhorn W, Dessen A, Calder LJ, Harrison SC, Skehel JJ & Wiley DC. Structural basis for membrane fusion by enveloped viruses. *Molecular Membrane Biology* 1999; 16:3–9.
- Wild C, Oas T, McDanal C, Bolognesi D & Matthews T. A synthetic peptide inhibitor of human immunodeficiency virus replication: correlation between solution structure and viral inhibition. *Proceedings of the National Academy of Sciences of the United States of America* 1992; 89:10537–10541.
- Jiang S, Lin K, Strick N & Neurath AR. HIV-1 inhibition by a peptide. *Nature* 1993; 365:113.
- Wild C, Greenwell T & Matthews T. A synthetic peptide from HIV-1 gp41 is a potent inhibitor of virus-mediated cell-cell fusion. *AIDS Research and Human Retroviruses* 1993; 9:1051–1053.
- Wild C, Shugars D, Greenwell T, McDanal C & Matthews T. Peptides corresponding to a predictive alpha-helical domain of human immunodeficiency virus type 1 gp41 are potent inhibitors of virus infection. *Proceedings of the National Academy of Sciences of the United States of America* 1994; 91:9770–9774.
- Roman F, Gonzalez D, Lambert C, Deroo S, Fischer A, Baurith T, Staub T, Boulme R, Arendt V, Schneider F, Hemmer R & Schmit JC. Uncommon mutations at residue positions critical for enfuvirtide (T-20) resistance in enfuvirtide-naïve patients infected with subtype B and non-B HIV-1 strains. *Journal of Acquired Immune Deficiency Syndromes* 2003; 33:134–139.
- Marcelin AG, Reynes J, Yerly S, Ktorza N, Segondy M, Piot JC, Delfraissy JF, Kaiser L, Perrin L, Katlama C & Calvez V. Characterization of genotypic determinants in HR-1 and HR-2 gp41 domains in individuals with persistent HIV viraemia under T-20. *AIDS* 2004; 18:1340–1342.
- Wei X, Decker JM, Liu H, Zhang Z, Arani RB, Kilby JM, Saag MS, Wu X, Shaw GM & Kappes JC. Emergence of resistant human immunodeficiency virus type 1 in patients receiving fusion inhibitor (T-20) monotherapy. *Antimicrobial Agents and Chemotherapy* 2002; 46:1896–1905.
- Lu J, Sista P, Giguel F, Greenberg M & Kuritzkes DR. Relative replicative fitness of human immunodeficiency virus type 1 mutants resistant to enfuvirtide (T-20). *Journal of Virology* 2004; 78:4628–4637.
- Menzo S, Castagna A, Monchetti A, Hasson H, Danise A, Carini E, Bagnarelli P, Lazzarin A & Clementi M. Genotype and phenotype patterns of human immunodeficiency virus type 1 resistance to enfuvirtide during long-term treatment. *Antimicrobial Agents and Chemotherapy* 2004; 48:3253–3259.
- Caffrey M. Model for the structure of the HIV gp41 ectodomain: insight into the intermolecular interactions of the gp41 loop. *Biochimica et Biophysica Acta* 2001; 1536:116–122.
- Bower M, Cohen FE & Dunbrack RL Jr. Prediction of protein side-chain rotamers from a backbone-dependent rotamer library: a new homology modeling tool. *Journal of Molecular Biology* 1997; 267:1268–1282.
- Levitt M & Lifson S. Refinement of protein conformations using a macromolecular energy minimization procedure. *Journal of Molecular Biology* 1969; 46:269–279.
- Levitt M. Energy refinement of hen egg-white lysozyme. *Journal of Molecular Biology* 1974; 82:393–420.
- Levitt M. Molecular dynamics of native protein. *Journal of Molecular Biology* 1983; 168:595–620.
- Levitt M, Hirshberg M, Sharon R & Daggett V. Potential energy function and parameters for simulations of the molecular dynamics of proteins and nucleic acids in solution. *Computer Physics Communications* 1995; 91:215–231.
- Samudrala R & Moult J. An all-atom distance dependent conditional probability discriminatory function for protein structure prediction. *Journal of Molecular Biology* 1997; 275:895–916.
- Hung LH, Ngan SC, Liu T & Samudrala R. PROTINFO: new algorithms for enhanced protein structure predictions. *Nucleic Acids Research* 2005; 33:77–80.
- Sanders RW, Vesanen M, Schuelke N, Master A, Schiffner L, Kalyanaraman R, Paluch M, Berkhout B, Maddon PJ, Olson WC, Lu M & Moore JP. Stabilization of the soluble, cleaved, trimeric form of the envelope glycoprotein complex of human immunodeficiency virus type 1. *Journal of Virology* 2002; 76:8875–8889.
- Markosyan RM, Ma X, Lu M, Cohen FS & Melikyan GB. The mechanism of inhibition of HIV1 env-mediated cell-cell fusion by recombinant cores of gp41 ectodomain. *Virology* 2002; 10:302:174–184.
- Greenberg ML & Cammack N. Resistance to enfuvirtide, the first HIV fusion inhibitor. *The Journal of Antimicrobial Chemotherapy* 2004; 54:333–340.
- Gallo SA, Sackett K, Rawat SS, Shai Y & Blumenthal R. The stability of the intact envelope glycoproteins is a major determinant of sensitivity of HIV/SIV to peptidic fusion inhibitors. *Journal of Molecular Biology* 2004; 340:9–14.